


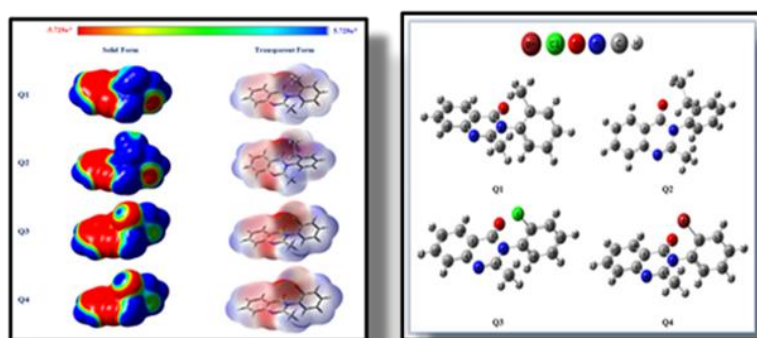
Full Paper | <http://dx.doi.org/10.17807/orbital.v15i5.18934>

# Quantum Chemical-Based Investigations and Lipophilicity Evaluations on Some Structurally Related Quinazoline Derivatives

Sümeyya Serin\* 

This work was chiefly conceived to explore the substituent effects on thermodynamic, electronic and lipophilic characteristics of some quinazoline derivatives (Q1-Q4) from theoretical aspects. The variations caused by methyl, ethyl, chlorine and bromine substituents on the same carbon of the aromatic ring were evaluated with a computational approach. In accordance with this purpose, simultaneously, DFT-based calculations were performed for vacuum and two different surroundings (DMSO and water) on methaqualone (Q1), etaqualone (Q2), mecloqualone (Q3), and mebroqualone (Q4) compounds by using the B3LYP functional and 6-311++G (d, p) split-valence triple zeta basis set. The computed thermodynamic quantities revealed that the halogen substitution was more preferable. The effect of substituent modification on electrostatic surface features was evaluated visually by molecular electrostatic potential (MEP) mapping technique. To shed light on the chemical reactivity behaviors of the Q1-Q4, DFT-based reactivity identifiers were computed. Also, the intramolecular interactions affected by substitution were evaluated on the basis of the Natural Bond Orbital (NBO) theory. The NBO results revealed that  $\pi$ - $\pi^*$  interactions predominate for each compound. The lipophilic character analyzes of the mentioned compounds were evaluated both numerically and visually. The data of both methods support each other.

## Graphical abstract



## Keywords

DFT study  
Lipophilicity  
NBO  
Quinazoline

## Article history

Received day month year  
Revised day month year  
Accepted day month year  
Available online day month year

Handling Editor: Arlan Gonçalves

## 1. Introduction

Heterocyclic compounds constitute an important group in all aspects of pure and applied chemistry, they also play a vital role in the field of medicinal chemistry, especially for the

therapy of diseases and infections [1-3]. Among this group, heterocycles containing quinazoline motif occupy a significant place due to their various biological activities [4-6].

As shown in Figure 1, quinazoline (1) is a pyrimidine compound and can be classified as quinazolin-2(1H)-one (2) and quinazolin-4(3H)-one (3) [7]. To date, a wide variety of

pharmacological activities of quinazoline derivatives have been reported (Figure 1) [8-10].

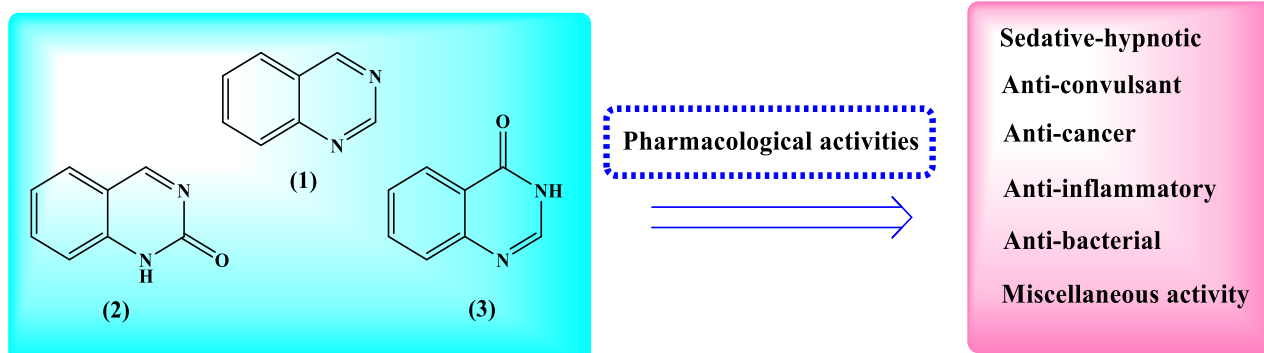


Fig. 1. Some pharmacological activities of quinazolines (1-3).

Table 1. Chemical representations, brand and IUPAC names of studied compounds

Molecular Structure	Brand name	IUPAC name
	(Q1) Methaqualone Quaalude	2-methyl-3-(2-methylphenyl) quinazolin-4-one
	(Q2) Etaqualone Aolan	3-(2-ethylphenyl)-2- methylquinazolin-4-one
	(Q3) Mecloqualone Nubarene, Casfen	3-(2-chlorophenyl)-2- methylquinazolin-4-one
	(Q4) Mebroqualone NSC-631646	3-(2-bromophenyl)-2- methylquinazolin-4-one

Lipophilic domain
  H-bond acceptor and electron donor
  Substituted domain

In particular, quinazoline and quinazolinone derivatives are among the most studied classes of compounds due to their anticonvulsant activities in recent years [11-13]. Methaqualone is a synthetic derivative that contains quinazoline core and is an important milestone in anticonvulsant activity [14]. Besides, many quinazoline derivatives structurally related to methaqualone were explored and examined for their anti-convulsant activities. A literature search has revealed the requirement for a methyl group at position 2 and a substituted aromatic ring at position 3 for anticonvulsant activity. However, it is emphasized that the synthesis of new derivatives free of hepatotoxicity and neurotoxicity by modification of the lipophilic pharmacophore at 3rd position of the quinazoline ring has gained importance. As a result of these modifications, new potent anticonvulsants have been developed and their bioactivities have been experimentally studied [15, 16]. However, it should be noted that small changes in the molecular structure also led to changes in physicochemical properties. Bioactivity can be regarded as a reflection of these physicochemical properties. Computational chemistry methods can contribute to the design of new drugs by identifying important interactions that can influence bioactivity. In particular, prediction of key parameters such as absorption, hydrophilicity, lipophilicity, and toxicity is of great advantage. In silico lipophilicity evaluations are also frequently encountered in the literature, since passage of the blood-brain barrier allowing potent anticonvulsant activity relies on the relatively high lipophilicity of the molecule. [17-20].

Taking all these into account, in the present study, methaqualone (Q1) and its three structurally similar derivatives, etaqualone (Q2), mecloqualone (Q3) and mebroqualone (Q4) compounds, were discussed from a quantum chemical point of view. The substituent effect on the aromatic ring was investigated by computational chemistry methods. The effects of substituent modification on thermodynamic parameters, quantum chemical reactivity descriptors, electrostatic surface properties (ESP) and intramolecular interactions were examined through DFT-based calculations. The molecular structures, brand names and IUPAC names of the compounds Q1-Q4 that are the subject of the present study are presented in Table 1. Also, the 3D molecular lipophilicity potential (MLP) maps that display the accumulative lipophilic contributions of each atom in studied derivatives were visualized. In addition to the quantum chemical explorations, numerical and visual evaluation of the lipophilic characters of the aforementioned compounds using SwissADME [21] and Molinspiration software [22, 23] highlights the original value of this study.

## 2. Material and Methods

### 2.1 Computational Methods

All optimization and frequency computations presented in the study were performed by using GAUSSIAN 16 software package [24] on applying the B3LYP functional and the 6-311++G (d, p) basis set to realize the optimized structures of Q1-Q4 [25-27]. Gauss View 6 software [28] was utilized for illustrations of the optimized structures, FMO, and MEP diagrams. To gain the density of states (DOS) plots, Gauss-Sum 3.0 [29] program was operated. The solvent phase calculations were carried out by using conductor-like polarizable continuum model (CPCM) [30]. DMSO ( $\epsilon=46.8$ ), and water ( $\epsilon=78.4$ ) environments were simulated by mentioned solvent model. For all computations, optimized

structures were verified by the absence of imaginary frequency. In order to evaluate basic physicochemical and lipophilicity characteristics of Q1-Q4, SwissADME software [21] was utilized. The n-octanol/water partition coefficients ( $\log P_{ow}$ ) were determined utilizing five methodologies, which were ILOGP, XLOGP3, WLOGP, MLOGP, and SILICOS-IT. Additionally, molecular lipophilicity potential (MLP) and topological polar surface area (TPSA) maps of studied molecules were visualized in Molinspiration Galaxy 3D Structure Generator v2018.01 beta [22, 23].

The thermochemical quantities,  $E_{vib}$ . (vibrational thermal energy),  $S_{vib}$ . (vibrational entropy), and  $Cv_{vib}$ . (vibrational heat capacity) of the studied molecules were calculated through specific equations ((1)-(5)) defined below in accordance with the principles of quantum mechanics [31-34]. The following explanations refer to the terms presented in the equations:  $\theta_{v,j}=hv_j/k \rightarrow$  vibrational temperature,  $k \rightarrow$  Boltzmann constant,  $h \rightarrow$  Planck constant, and  $v_j \rightarrow j^{th}$  fundamental frequency.

$$Q = Q_{trans.} \times Q_{rot.} \times Q_{vib.} Q_{elec.} \quad (1)$$

$$Q_{vib.} = \prod_{j=1}^{3N-6} \frac{e^{-\theta_{v,j}/2T}}{\left(1 - e^{-\frac{\theta_{v,j}}{T}}\right)} \quad (2)$$

$$E_{vib.} = Nk \sum_{j=1}^{3N-6} \left( \frac{\theta_{v,j}}{2} + \frac{\theta_{v,j} e^{-\theta_{v,j}/T}}{\left(1 - e^{-\frac{\theta_{v,j}}{T}}\right)} \right) \quad (3)$$

$$S_{vib.} = Nk \sum_{j=1}^{3N-6} \left[ \frac{\theta_{v,j}/T}{\left(e^{\theta_{v,j}/T} - 1\right)} - \ln \left(1 - e^{-\theta_{v,j}/T}\right) \right] \quad (4)$$

$$Cv_{vib.} = Nk \sum_{j=1}^{3N-6} \left[ \left(\frac{\theta_{v,j}}{T}\right)^2 \frac{e^{\theta_{v,j}/T}}{\left(e^{\theta_{v,j}/T} - 1\right)^2} \right] \quad (5)$$

According to Koopmans theorem [35], ionization energy ( $I$ ) ( $I = -E_{HOMO}$ ) and electron affinity ( $A$ ) ( $A = -E_{LUMO}$ ) values can be defined by Highest Occupied Molecular Orbital (HOMO) and Lowest Unoccupied Molecular Orbital (LUMO) energies. Moreover, some DFT-based reactivity parameters such as chemical hardness ( $\eta$ ), chemical potential ( $\mu$ ), electronegativity ( $\chi$ ), and electrophilicity index ( $\omega$ ), as well as frontier molecular orbital energies ( $E_{HOMO}$  and  $E_{LUMO}$ ), which are subjected to the calculation of energy gap values ( $\Delta E$ ;  $\Delta E = E_{LUMO} - E_{HOMO}$ ), are presented in the equations below ((6)-(9)) [36-40].

$$\text{Chemical Potential} \quad \mu = -\frac{I + A}{2} \quad (6)$$

$$\text{Chemical Hardness} \quad \eta = \frac{I - A}{2} \quad (7)$$

$$\text{Electronegativity} \quad \chi = \frac{I + A}{2} \quad (8)$$

$$\text{Electrophilicity index} \quad \omega = \frac{\mu^2}{2\eta} \quad (9)$$

NBO analyses of the Q1-Q4 compounds were carried out utilizing the second-order Fock matrix [41, 42] at DFT/B3LYP/6-311++G (d, p) methodology. In this way, donor-acceptor orbital interactions and stabilization energy

predictions were defined. Stabilization energy values were calculated according to the formula specified in equation (10). The terms in the formula are expressed as follows:  $E^{(2)}$ : Stabilization energy,  $q_i$ : Donor orbital occupancy,  $F_{ij}$ : Off diagonal Fock matrix,  $\epsilon_i$  and  $\epsilon_j$ : diagonal element, donor and acceptor orbital energies.

$$E^{(2)} = \Delta E_{ij} = q_i \left[ \frac{(F_{ij})^2}{(\epsilon_j - \epsilon_i)} \right] \quad (10)$$

### 3. Results and Discussion

#### 3.1 Optimized Geometry

B3LYP/6-311++G (d, p) theory-level optimized structures of Q1-Q4 are depicted in Figure 2 with labeling and numbering scheme. Theoretical bond length and bond angle values of the compounds were checked with the experimental values given in reference [43]. Accordingly, while the theoretical C=O bond length for all four derivatives was determined as 1.22 Å, this value was experimentally reported as 1.20 Å. For Q1 and Q2, the C7-N2 bond length is theoretically predicted to be 1.42 Å

and experimentally determined to be 1.40 Å. This bond corresponds to the C7-N3 bond in compounds Q3 and Q4 and was similarly calculated as 1.42 Å. Similarly, N2-C4 (for Q1 and Q2) and N3-C8 (for Q3 and Q4) bond lengths were calculated as 1.45 Å and 1.44 Å, respectively. Experimental data expresses the relevant bond length as 1.46 Å. While aromatic ring C-C bond lengths are calculated to be in the range of 1.38-1.41 Å, they have been experimentally reported in the range of 1.36-1.40 Å. When it comes to bond angles, for Q1 and Q2, the O1-C7-N2 bond angle was calculated as 120.7° and 120.8°, respectively, while the O2-C7-N3 bond angle corresponding to this angle in Q3 and Q4 compounds was calculated as 120.6° for both compounds. The experimental value of the relevant angle was determined as 120.8°. Besides, for Q1 and Q2, the C7-N2-C4 angle was calculated as 116.8° and 116.9°, respectively, while for Q3 and Q4, the C7-N3-C8 angle was calculated as 116.2° and 116.3°. The experimental bond angle is stated as 116.6°. While aromatic ring C-C-C bond angles for the studied compounds were computed in the range of 117.4-121.5°, they were experimentally reported in the range of 118.4-122.0°. Therefore, it is clearly seen that the experimental and theoretical data are quite compatible with each other in terms of both bond lengths and bond angles.

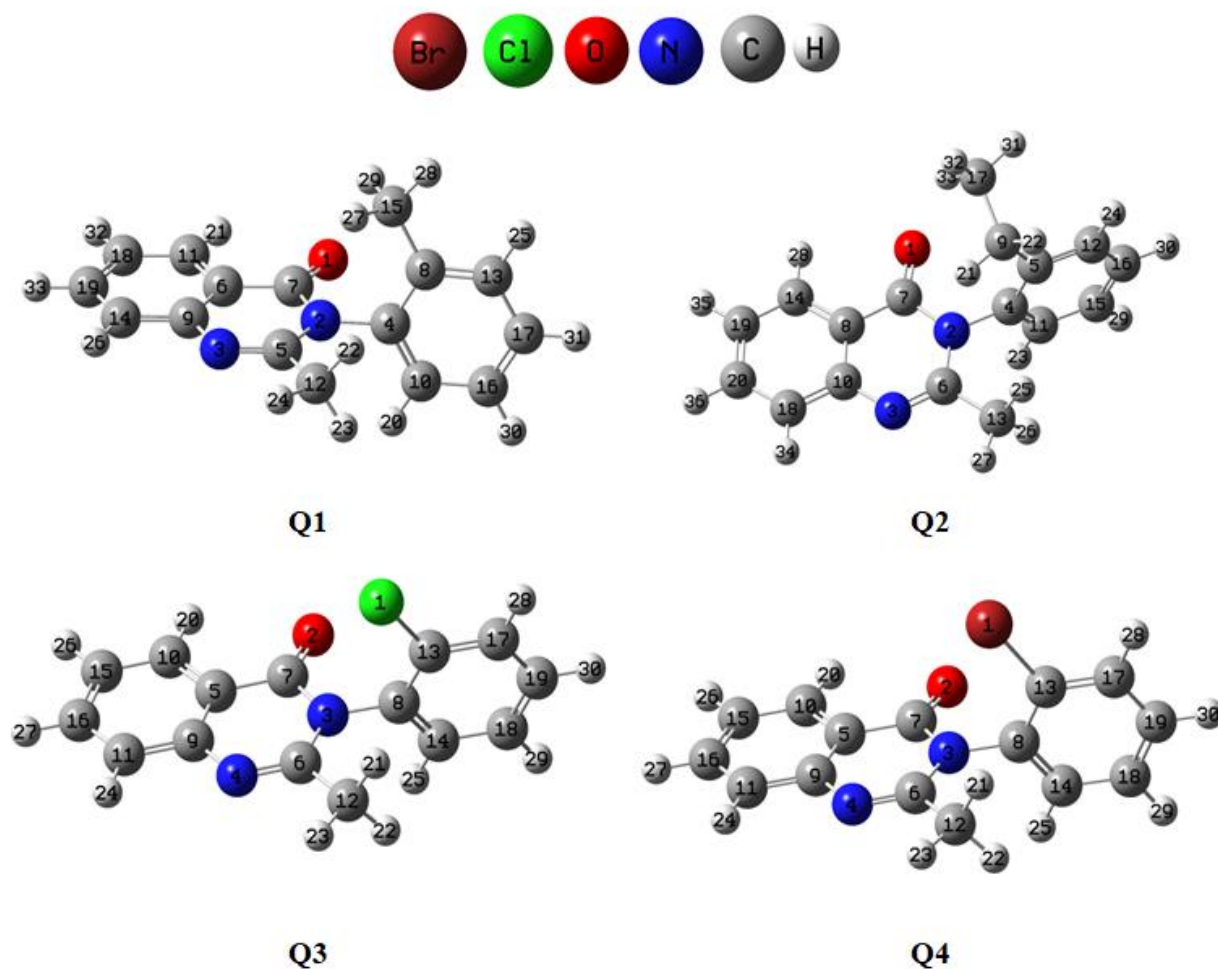


Fig. 2. DFT-Optimized Molecular Structures of Q1-Q4.

#### 3.2 Thermodynamic Parameters

The computed thermodynamic and physicochemical characteristics of the studied Q1-Q4 compounds and their variations according to the solvent environment are listed in

Table 2. As can be clearly seen from Table 2, it was observed that the dipole moment ( $DM, D$ ) values for each compound increased in the solvent phases. The same trend applies to polarizability ( $\alpha$ , a.u.). The dipole moment values calculated

for the water phase were listed as Q3 (3.952 D) > Q4 (3.878 D) > Q2 (3.070 D) > Q1 (3.062 D), while the polarizability values for the same phase were calculated as Q2 (303.482 a.u.) > Q4 (299.788 a.u.) > Q3 (287.681 a.u.) > Q1 (286.877 a.u.). It can be said that all studied compounds are more polarized in aqueous media.

Considering thermodynamic state functions  $\Delta E$  (total energy),  $\Delta H$  (enthalpy), and  $\Delta G$  (free energy) quantities, the following sequence was obtained for the water phase calculations of each compound:

$\Delta E$  (a.u.): Q1 (-802.8421) > Q2 (-842.1348) > Q3 (-

1223.1719) > Q4 (-3337.0917)

$\Delta H$  (a.u.): Q1 (-802.8412) > Q2 (-842.1339) > Q3 (-1223.1710) > Q4 (-3337.0907)

$\Delta G$  (a.u.): Q1 (-802.9010) > Q2 (-842.1967) > Q3 (-1223.2305) > Q4 (-3337.1514)

The decrease in the values of the thermodynamic state functions with the substitution of the ethyl group for the methyl group in the aromatic ring is less than that due to chlorine or bromine substitution. Therefore, it can be said that halogen substitution is preferable.

**Table 2.** The computed thermodynamic and physicochemical characteristics of Q1-Q4

	Q1	Vacuum	DMSO	Water	Q2	Vacuum	DMSO	Water
<i>DM</i> (Debye)		2.073	3.049	3.062	<i>DM</i> (Debye)	2.019	3.056	3.070
$\alpha$ (a.u.)		206.737	285.883	286.877	$\alpha$ (a.u.)	218.659	302.429	303.482
$\Delta E$ (a.u.)		-802.8297	-802.8420	-802.8421	$\Delta E$ (a.u.)	-842.1227	-842.1347	-842.1348
$\Delta H$ (a.u.)		-802.8288	-802.8410	-802.8412	$\Delta H$ (a.u.)	-842.1217	-842.1337	-842.1339
$\Delta G$ (a.u.)		-802.8887	-802.9009	-802.9010	$\Delta G$ (a.u.)	-842.1848	-842.1966	-842.1967
$\Delta E_{thermal}$ (kcal/mol)		174.898	174.778	174.777	$\Delta E_{thermal}$ (kcal/mol)	193.704	193.560	193.558
$\Delta E_{vib.}$ (kcal/mol)		173.121	173.001	172.999	$\Delta E_{vib.}$ (kcal/mol)	191.926	191.782	191.781
<i>Cv</i> (cal/molK)		61.881	61.866	61.866	<i>Cv</i> (cal/molK)	66.621	66.611	66.611
<i>Cv<sub>vib.</sub></i> (cal/molK)		55.920	55.905	55.905	<i>Cv<sub>vib.</sub></i> (cal/molK)	60.660	60.650	60.650
<i>S</i> (cal/molK)		126.230	125.879	125.881	<i>S</i> (cal/molK)	132.643	132.322	132.315
<i>S<sub>vib.</sub></i> (cal/molK)		50.680	50.329	50.331	<i>S<sub>vib.</sub></i> (cal/molK)	56.563	56.238	56.231
	Q3	Vacuum	DMSO	Water	Q4	Vacuum	DMSO	Water
<i>DM</i> (Debye)		2.701	3.935	3.952	<i>DM</i> (Debye)	2.631	3.861	3.878
$\alpha$ (a.u.)		206.923	286.680	287.681	$\alpha$ (a.u.)	214.288	298.721	299.788
$\Delta E$ (a.u.)		-1223.1592	-1223.1718	-1223.1719	$\Delta E$ (a.u.)	-3337.0788	-3337.0915	-3337.0917
$\Delta H$ (a.u.)		-1223.1583	-1223.1709	-1223.1710	$\Delta H$ (a.u.)	-3337.0777	-3337.0906	-3337.0907
$\Delta G$ (a.u.)		-1223.2178	-1223.2303	-1223.2305	$\Delta G$ (a.u.)	-3337.1387	-3337.1513	-3337.1514
$\Delta E_{thermal}$ (kcal/mol)		151.350	151.266	151.264	$\Delta E_{thermal}$ (kcal/mol)	151.102	151.015	151.015
$\Delta E_{vib.}$ (kcal/mol)		149.573	149.488	149.487	$\Delta E_{vib.}$ (kcal/mol)	149.324	149.238	149.237
<i>Cv</i> (cal/molK)		59.727	59.709	59.710	<i>Cv</i> (cal/molK)	60.188	60.173	60.172
<i>Cv<sub>vib.</sub></i> (cal/molK)		53.766	53.748	53.748	<i>Cv<sub>vib.</sub></i> (cal/molK)	54.226	54.211	54.211
<i>S</i> (cal/molK)		125.315	125.158	125.154	<i>S</i> (cal/molK)	128.014	127.818	127.809
<i>S<sub>vib.</sub></i> (cal/molK)		49.229	49.074	49.070	<i>S<sub>vib.</sub></i> (cal/molK)	50.993	50.799	50.790

### 3.3 FMO and MEP Analysis

In order to shed light on the chemical reactivity behaviors and reactive sites of the mentioned Q1-Q4 compounds, frontier molecular orbital computations and MEP mapping techniques were utilized. FMO analysis is an important phenomenon in computational chemistry, as some parameters such as electronic absorption, chemical hardness, and chemical softness are associated with HOMO-LUMO transitions and energy values. The energy gap value ( $\Delta E = E_{LUMO} - E_{HOMO}$ ) of a particular molecule plays a substantial role in the chemical stability and reactivity evaluations of that molecule [44]. In this context, the quantum chemical reactivity descriptors obtained as a result of the calculations for the vacuum and solvent phases at the B3LYP/6-311++G (d, p) theory level for the related compounds are represented in Table 3. As indicated in Table 3, the values of compounds Q1 and Q2 containing methyl and ethyl substituents on the aromatic ring were calculated close to each other. Similarly, the calculated values of the compounds Q3 and Q4 containing Cl and Br substituents on the aromatic ring are very close to each other. The energy gap values of the gas phase are as follows: Q3 (5.005 eV) > Q4 (5.003 eV) > Q2 (4.993 eV) > Q1 (4.992 eV). A low  $\Delta E$  value indicates low stability and high reactivity due to the easy transition of electrons. As expected, the chemical hardness values ( $\eta$ , eV) also show the same trend: Q3 (2.502 eV) = Q4 (2.502 eV) > Q2 (2.497 eV) > Q1 (2.496 eV). Taking chemical potential values ( $\mu$ , eV) into account, in each phase studied, the lowest values were calculated as -4.006 eV (vacuum), -4.233 eV (DMSO), and -

4.236 eV (water) for compound Q3. It is obvious that the computed DFT-based reactivity identifiers support each other.

Electron density distributions on HOMOs and LUMOs of Q1-Q4 and DOS graphs simulated with Gauss-Sum software [29] are exhibited in Figure 3 and Figure 4. In respect of Figure 3, it is noteworthy that the HOMO and LUMO amplitudes of all compounds are quite similar to each other. The HOMO & LUMO densities for all compounds were concentrated on the quinazolinone moiety. It is observed that LUMOs have antibonding character. It can be concluded that in vacuum, the substituents on the aromatic ring do not cause changes on the HOMO-LUMO electron densities.

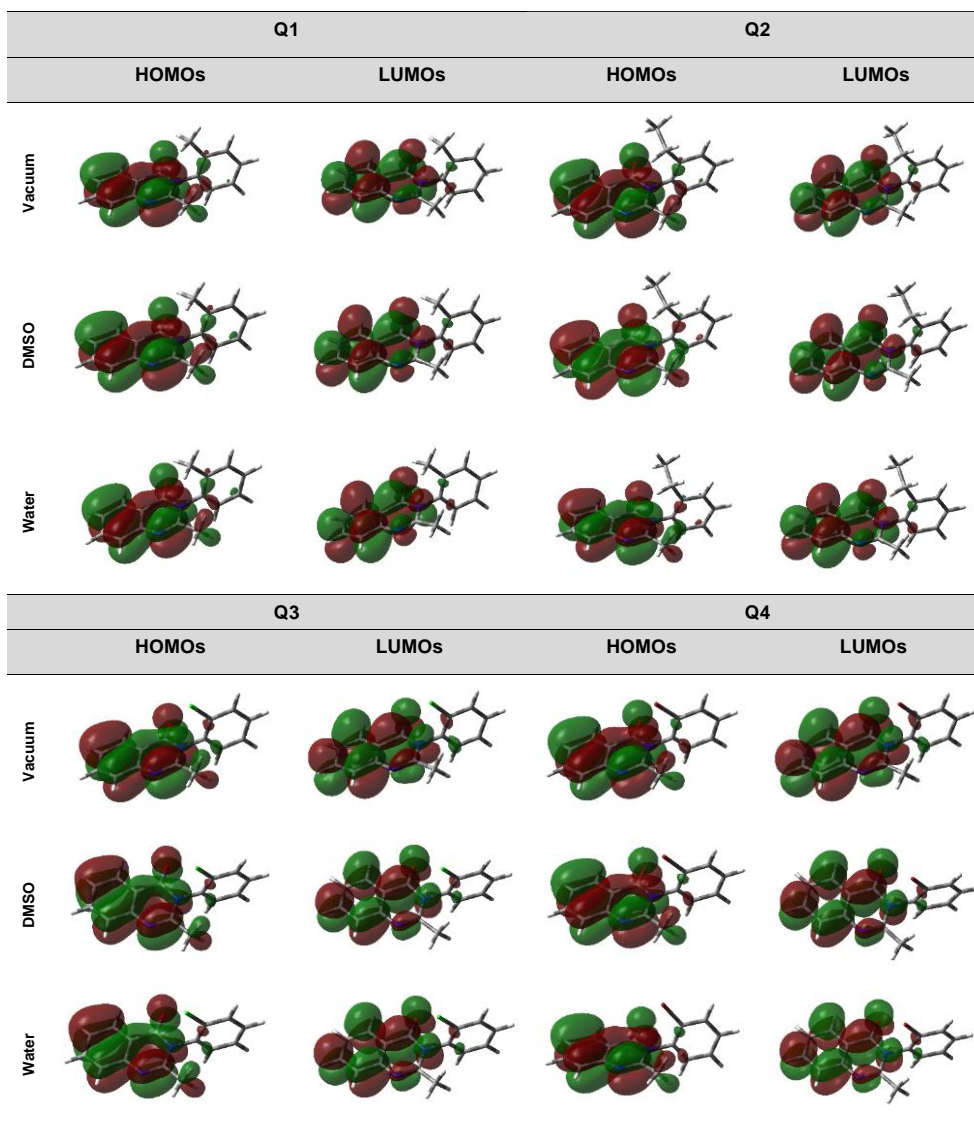
Molecular electrostatic potential (MEP) mapping is a method that uses color codes to provide an easy to figure out visualization of the charge distribution in a particular molecule [45, 46]. MEP maps have been visualized in order to clearly see the differences caused by different substituents on the same carbon atom of the aromatic ring in the electrostatic surface properties of the Q1-Q4 compounds. The use of the same level of theory and the same visual phenomenon is an important factor in order to make a consistent comparison. Visualized MEP maps in both solid and transparent form for Q1-Q4 compounds are shown in Figure 5. At the same time, MEP surfaces created using DMSO and water solvents are also included in Figure 5. The molecular electrostatic potentials of mentioned compounds are in the range of -0.005729 a.u. (deepest red) - +0.005729 a.u. (deepest blue) in each phase. Generally, on the color scale of MEP maps, red designates

high electron density, blue designates low electron density, and yellow and green designate intermediate levels. Accordingly, for each compound, a larger amount of electron density is on the quinazolinone ring and predominantly red shading is present (intense red caused by the  $\pi$ -electron cloud induced by the aromatic system). In addition, a lower amount of electron density was observed at the hydrogen

surroundings and predominantly blue shading is present. The MEP map of compound Q1 is similar to that of compound Q2, while the MEP map of compound Q3 is similar to that of compound Q4. Similar images emerged on MEP surfaces created in both vacuum and solvent environments for the same compound. Atoms have been shown to have the same negative (electrophilic) and positive (nucleophilic) potential.

**Table 3.** The quantum chemical reactivity parameters of the compounds Q1-Q4 (in eV)

Q1	$E_{HOMO}$	$E_{LUMO}$	$\Delta E$	$\eta$	$\mu$	$\chi$	$\omega$
Vacuum	-6.461	-1.469	4.992	2.496	-3.965	3.965	3.149
DMSO	-6.665	-1.690	4.975	2.488	-4.177	4.177	3.507
Water	-6.667	-1.692	4.975	2.487	-4.180	4.180	3.512
Q2	$E_{HOMO}$	$E_{LUMO}$	$\Delta E$	$\eta$	$\mu$	$\chi$	$\omega$
Vacuum	-6.462	-1.469	4.993	2.497	-3.966	3.966	3.149
DMSO	-6.660	-1.684	4.975	2.488	-4.172	4.172	3.498
Water	-6.662	-1.687	4.975	2.488	-4.175	4.175	3.503
Q3	$E_{HOMO}$	$E_{LUMO}$	$\Delta E$	$\eta$	$\mu$	$\chi$	$\omega$
Vacuum	-6.508	-1.503	5.005	2.502	-4.006	4.006	3.206
DMSO	-6.724	-1.742	4.983	2.491	-4.233	4.233	3.596
Water	-6.727	-1.745	4.982	2.491	-4.236	4.236	3.601
Q4	$E_{HOMO}$	$E_{LUMO}$	$\Delta E$	$\eta$	$\mu$	$\chi$	$\omega$
Vacuum	-6.504	-1.501	5.003	2.502	-4.003	4.003	3.203
DMSO	-6.722	-1.742	4.981	2.490	-4.232	4.232	3.596
Water	-6.725	-1.745	4.981	2.490	-4.235	4.235	3.601



**Fig. 3.** HOMO & LUMO plots (isoval: 0.02 a.u.) of Q1-Q4 for each phase.

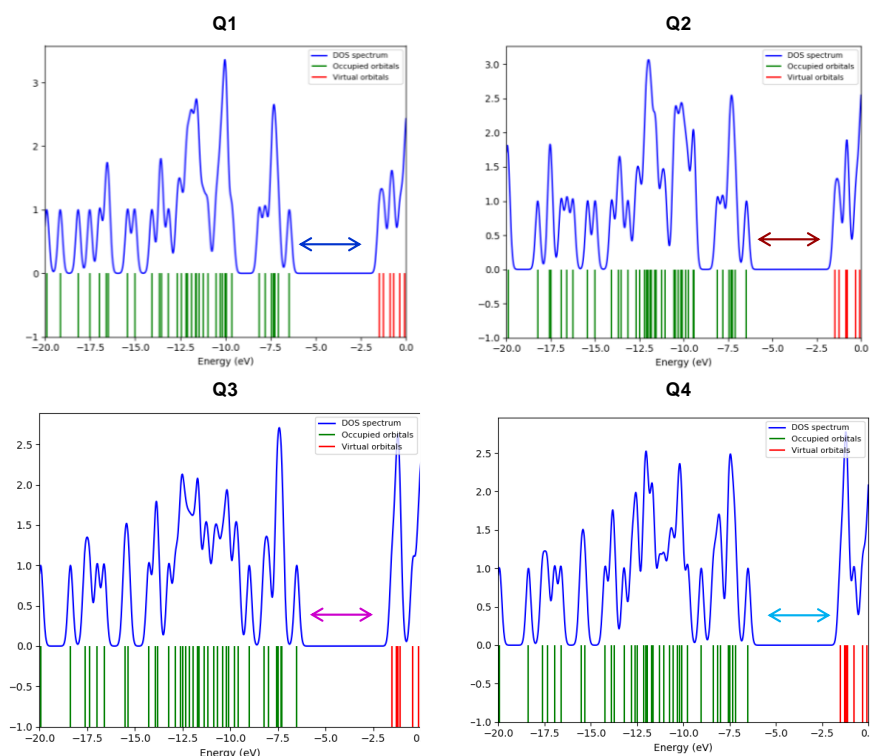


Fig. 4. DOS diagrams of Q1-Q4.

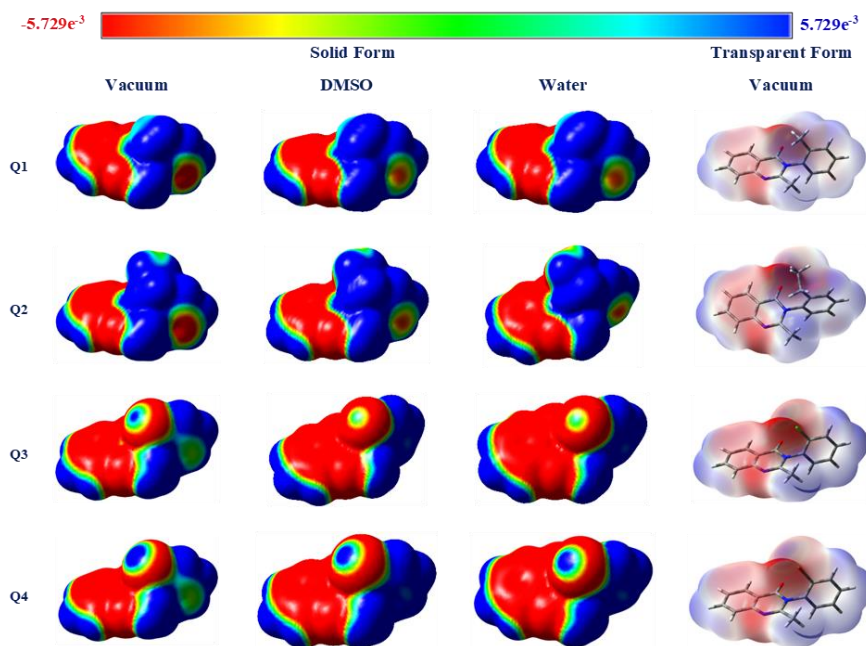


Fig. 5. MEP maps (isoval: 0.0004 a.u.) of Q1-Q4.

### 3.4 Lipophilic Character Analysis

One of the important steps of drug design studies is to examine the absorption, distribution, metabolism and excretion (ADME) processes of the drug candidate in the body. One of the main factors affecting this process is lipophilicity. It is important to establish the hydrophilic-lipophilic balance of the drug candidate in order for the process to proceed in a healthy way [47]. In this manner, estimating the critical parameters of the drug candidate by using computational chemistry methods while still in the design phase provides an advantage to speed up the process. In this part of the study, *in silico* lipophilic character analysis

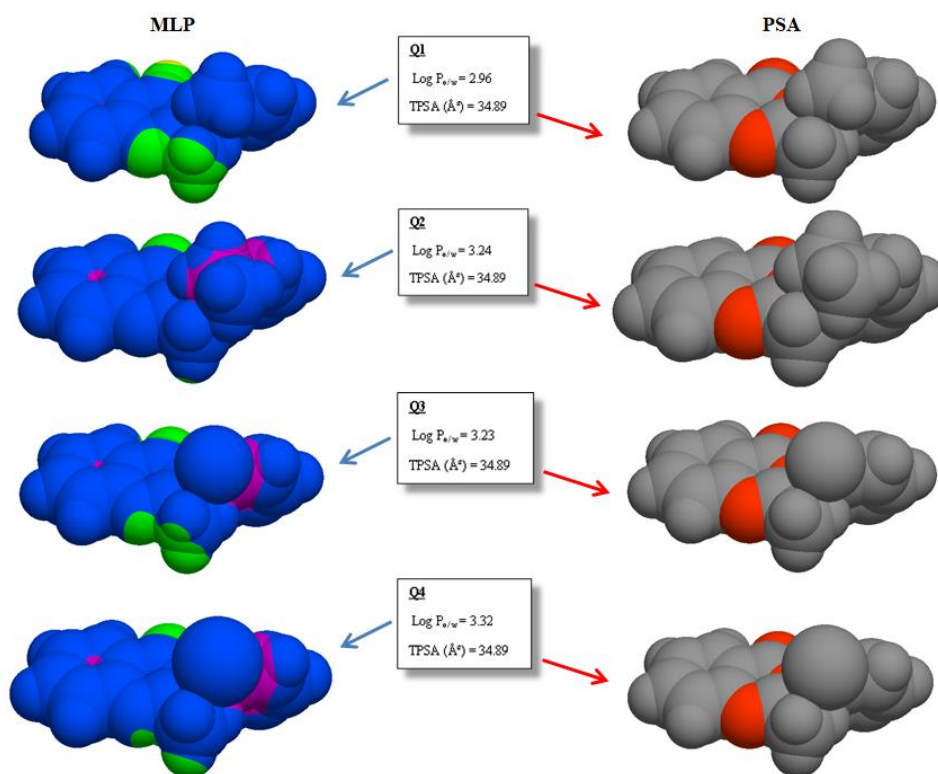
was performed for the mentioned quinazolinone compounds Q1-Q4. To this end, SwissADME and Molinspiration software were utilized. Both web tools are freely accessible and easy to use. Table 4 implicates numerical estimates of the physicochemical and lipophilic properties of Q1-Q4. As demonstrated in Table 4, physicochemical properties are similar for all studied compounds. Since the numbers of H-bond donors and H-bond acceptors are the same, the topological polar surface area (TPSA) values were calculated as 34.89 Å<sup>2</sup> for all molecules. This situation is supported by the polar surface area maps obtained via Molinspiration software and visualized in Figure 6. In PSA maps, gray color

designates non-polar regions and red color designates polar regions. It was observed that the red colored regions were the same in all compounds. Therefore, it can be concluded that methyl, ethyl, chlorine and bromine substituents attached to the same carbon atom of the aromatic ring have no effect on the polar surface area. In the case of lipophilic character analysis, iLOGP, XLOGP3, WLOGP, MLOGP, and SILICOS-IT [48-52] predictive models are taken into account via SwissADME software. The arithmetic average of whole models is presented as consensus  $\log P_{ow}$ . For Q1-Q4,  $\log P_{ow}$  values, the numerical expression of lipophilicity, gave different results in each predictive model. The order of average  $\log P_{ow}$  of Q1-Q4 was determined as Q4 (3.32) > Q2 (3.24) > Q3 (3.23) > Q1 (2.96). The calculated  $\log P_{ow}$  values ( $\log P_{ow} > 2.0$ ) revealed that all studied compounds could exhibit lipophilic character. As expected, the  $\log P_{ow}$  value increased depending on the chain length with the substitution of the methyl group

with the ethyl group. Similarly, the  $\log P$  value increased as a result of the substitution of chlorine with larger bromine. As with polar surface area assessment, lipophilicity results can be supplemented with molecular lipophilicity potential (MLP) maps obtained via Molinspiration software, as shown in Figure 6. Color codes were used in MLP maps. Orange/red regions designate hydrophilic surfaces while violet/blue regions designate the most lipophilic surfaces. Last, regions coded in yellow/green point out intermediate lipophilic surfaces. It is evident that the blue and violet zones representing the lipophilic surfaces are highly intense in all compounds. When the MLP maps of the compounds Q1-Q2 and Q3-Q4 are compared among themselves, it is expected that Q2 will be slightly more lipophilic than Q1 and Q4 to be slightly more lipophilic than Q3. At this point, it is obvious that both SwissADME and Molinspiration analysis results support each other.

**Table 4.** Estimations of physicochemical properties and  $\log P_{ow}$  values for Q1-Q4

Physicochemical properties	Q1	Q2	Q3	Q4
Formula	C <sub>16</sub> H <sub>14</sub> N <sub>2</sub> O	C <sub>17</sub> H <sub>16</sub> N <sub>2</sub> O	C <sub>15</sub> H <sub>11</sub> ClN <sub>2</sub> O	C <sub>15</sub> H <sub>11</sub> BrN <sub>2</sub> O
Molecular weight (g/mol)	250.30	264.32	270.71	315.16
Num. heavy atoms	19	20	19	19
Num. arom. heavy atoms	16	16	16	16
Fraction Csp <sup>3</sup>	0.12	0.18	0.07	0.07
Num. rotatable bonds	1	2	1	1
Num. H-bond acceptors	2	2	2	2
Num. H-bond donors	0	0	0	0
Molar Refractivity	77.27	82.08	77.32	80.01
TPSA (Å <sup>2</sup> )	34.89	34.89	34.89	34.89
<b>Lipophilicity</b>				
Log P <sub>ow</sub> (iLOGP)	2.76	2.89	2.73	2.81
Log P <sub>ow</sub> (XLOGP3)	2.50	2.93	2.76	2.83
Log P <sub>ow</sub> (WLOGP)	3.00	3.26	3.35	3.46
Log P <sub>ow</sub> (MLOGP)	2.99	3.24	3.67	3.79
Log P <sub>ow</sub> (SILICOS-IT)	3.53	3.89	3.66	3.69
Consensus Log P <sub>ow</sub>	2.96	3.24	3.23	3.32



**Fig. 6.** 3D CPK view of MLP and PSA maps for Q1-Q4



### 3.5 NBO Analysis

Today, NBO computations are frequently used in various molecular systems to study charge transfer, electronic transitions, and possible donor-acceptor interactions. Therefore, in this part of the work, NBO analyzes of Q1-Q4 compounds were performed by using same theory level. The data obtained in line with the analysis outputs are summarized in Table 5. From Table 5, it is evident that the  $\pi$ - $\pi^*$  interactions are predominant for each compound. The stabilization energies calculated for the  $\pi$ - $\pi^*$  interactions of Q1, Q2, Q3, and Q4 compounds vary in the range of 14.95-26.08 kcal/mol, 14.35-26.14 kcal/mol, 15.04-25.46 kcal/mol, and 15.00-25.87 kcal/mol, respectively. Taking LP- $\pi^*$  interactions into account, stabilization energy values of LP (1) N2 ( $ED_i = 1.60935e$ )  $\rightarrow$   $\pi^*$  O1-C7 ( $ED_j = 0.31207e$ ) and LP (1)

N2 ( $ED_i = 1.60935e$ )  $\rightarrow$   $\pi^*$  N3-C5 ( $ED_j = 0.26933e$ ) were computed as 46.57 and 47.62 kcal/mol for Q1, respectively. Similarly, the stabilization energies of LP (1) N2 ( $ED_i = 1.60937e$ )  $\rightarrow$   $\pi^*$  O1-C7 ( $ED_j = 0.31353e$ ) and LP (1) N2 ( $ED_i = 1.60937e$ )  $\rightarrow$   $\pi^*$  N3-C6 ( $ED_j = 0.26876e$ ) in compound Q2 were calculated as 46.79 and 47.39 kcal/mol, respectively. Similar interactions were also observed in compounds Q3 and Q4, but with a slight decrease in energy values. However, the interactions of lone pairs of Cl1 and Br1 with  $\pi^*$  C8-C13 antibonding orbitals were concerned. While LP (3) Cl1 ( $ED_i = 1.92302e$ )  $\rightarrow$   $\pi^*$  C8-C13 ( $ED_j = 0.42036e$ ) interaction stabilized the molecule with an energy value of 13.37 kcal/mol in compound Q3, LP (3) Br1 ( $ED_i = 1.93144e$ )  $\rightarrow$   $\pi^*$  C8-C13 ( $ED_j = 0.41687e$ ) interaction stabilized the molecule with an energy value of 10.54 kcal/mol in compound Q4.

**Table 5.** NBO analysis outputs of Q1-Q4 at B3LYP/6-311++G (d, p) theory level

Q1	Donor(i)	ED <sub>i</sub> /e	Acceptor(j)	ED <sub>j</sub> /e	E <sup>(2)</sup> kcal/mol	E(j)-E(i)/a.u	F(i,j)/a.u
	$\pi$ N3-C5	1.86149	$\pi^*$ C6-C9	0.42251	18.15	0.35	0.077
	$\pi$ C4-C10	1.68306	$\pi^*$ C8-C13	0.33241	21.11	0.30	0.071
			$\pi^*$ C16-C17	0.33104	17.93	0.30	0.066
	$\pi$ C6-C9	1.60255	$\pi^*$ O1-C7	0.31207	26.08	0.27	0.076
			$\pi^*$ C11-C18	0.27302	19.57	0.29	0.069
			$\pi^*$ C14-C19	0.27444	14.95	0.29	0.061
	$\pi$ C8-C13	1.63551	$\pi^*$ C4-C10	0.36110	21.13	0.28	0.068
			$\pi^*$ C16-C17	0.33104	21.50	0.29	0.071
	$\pi$ C11-C18	1.68617	$\pi^*$ C6-C9	0.42251	17.29	0.28	0.064
			$\pi^*$ C14-C19	0.27444	19.89	0.29	0.068
	$\pi$ C14-C19	1.69261	$\pi^*$ C6-C9	0.42251	20.56	0.28	0.070
			$\pi^*$ C11-C18	0.27302	16.99	0.29	0.063
	$\pi$ C16-C17	1.66037	$\pi^*$ C4-C10	0.36110	21.85	0.28	0.070
			$\pi^*$ C8-C13	0.33241	19.09	0.29	0.066
	LP (1) N2	1.60935	$\pi^*$ O1-C7	0.31207	46.57	0.29	0.105
			$\pi^*$ N3-C5	0.26933	47.62	0.29	0.108
Q2	Donor(i)	ED <sub>i</sub> /e	Acceptor(j)	ED <sub>j</sub> /e	E <sup>(2)</sup> kcal/mol	E(j)-E(i)/a.u	F(i,j)/a.u
	$\pi$ N3-C6	1.86119	$\pi^*$ C8-C10	0.42253	18.18	0.35	0.077
	$\pi$ C4-C5	1.66115	$\pi^*$ C11-C15	0.32219	21.73	0.29	0.071
			$\pi^*$ C12-C16	0.31822	18.13	0.29	0.065
	$\pi$ C8-C10	1.60259	$\pi^*$ O1-C7	0.31353	26.14	0.27	0.076
			$\pi^*$ C14-C19	0.27294	19.58	0.29	0.069
			$\pi^*$ C18-C20	0.27427	14.35	0.30	0.061
	$\pi$ C11-C15	1.66461	$\pi^*$ C4-C5	0.36348	19.87	0.29	0.068
			$\pi^*$ C12-C16	0.31822	20.59	0.28	0.069
	$\pi$ C12-C16	1.67019	$\pi^*$ C4-C5	0.36348	21.73	0.29	0.071
			$\pi^*$ C11-C15	0.32219	19.45	0.28	0.066
	$\pi$ C14-C19	1.68627	$\pi^*$ C8-C10	0.42253	17.28	0.28	0.064
			$\pi^*$ C18-C20	0.27427	19.05	0.30	0.068
	$\pi$ C18-C20	1.69260	$\pi^*$ C8-C10	0.42253	20.53	0.28	0.070
			$\pi^*$ C14-C19	0.27294	17.00	0.29	0.063
	LP (1) N2	1.60937	$\pi^*$ O1-C7	0.31353	46.79	0.29	0.105
			$\pi^*$ N3-C6	0.26876	47.39	0.29	0.107
Q3	Donor(i)	ED <sub>i</sub> /e	Acceptor(j)	ED <sub>j</sub> /e	E <sup>(2)</sup> kcal/mol	E(j)-E(i)/a.u	F(i,j)/a.u
	$\pi$ N4-C6	1.86370	$\pi^*$ C5-C9	0.42248	17.97	0.35	0.077
	$\pi$ C5-C9	1.60281	$\pi^*$ O2-C7	0.30515	25.46	0.27	0.076
			$\pi^*$ C10-C15	0.27293	19.62	0.29	0.069
			$\pi^*$ C11-C16	0.27484	15.04	0.29	0.061
	$\pi$ C8-C13	1.68802	$\pi^*$ C14-C18	0.31657	18.78	0.31	0.068
			$\pi^*$ C17-C19	0.31815	17.57	0.32	0.067
	$\pi$ C10-C15	1.68411	$\pi^*$ C5-C9	0.42248	17.38	0.28	0.064
			$\pi^*$ C11-C16	0.27484	19.98	0.29	0.068
	$\pi$ C11-C16	1.69010	$\pi^*$ C5-C9	0.42248	20.67	0.28	0.070
			$\pi^*$ C10-C15	0.27293	17.05	0.29	0.063
	$\pi$ C14-C18	1.65282	$\pi^*$ C8-C13	0.42036	22.48	0.26	0.070
			$\pi^*$ C17-C19	0.31815	20.28	0.29	0.069
	$\pi$ C17-C19	1.66180	$\pi^*$ C8-C13	0.42036	21.70	0.27	0.069
			$\pi^*$ C14-C18	0.31657	19.05	0.29	0.066
	LP (3) Cl1	1.92302	$\pi^*$ C8-C13	0.42036	13.37	0.32	0.065
	LP (1) N3	1.62252	$\pi^*$ O2-C7	0.30515	44.88	0.29	0.104
			$\pi^*$ N4-C6	0.26173	46.11	0.29	0.107
Q4	Donor(i)	ED <sub>i</sub> /e	Acceptor(j)	ED <sub>j</sub> /e	E <sup>(2)</sup> kcal/mol	E(j)-E(i)/a.u	F(i,j)/a.u
	$\pi$ N4-C6	1.86367	$\pi^*$ C5-C9	0.42239	17.97	0.35	0.077
	$\pi$ C5-C9	1.60271	$\pi^*$ O2-C7	0.30516	25.87	0.27	0.076

		$\pi^*$ C10-C15	0.27297	19.56	0.29	0.069
		$\pi^*$ C11-C16	0.27490	15.00	0.29	0.061
$\pi$ C8-C13	1.69051	$\pi^*$ C14-C18	0.31529	18.53	0.31	0.067
		$\pi^*$ C17-C19	0.31643	17.71	0.32	0.067
$\pi$ C10-C15	1.68414	$\pi^*$ C5-C9	0.42239	17.37	0.28	0.064
		$\pi^*$ C11-C16	0.27490	19.97	0.29	0.068
$\pi$ C11-C16	1.69017	$\pi^*$ C5-C9	0.42239	20.65	0.28	0.070
		$\pi^*$ C10-C15	0.27297	17.01	0.29	0.063
$\pi$ C14-C18	1.65214	$\pi^*$ C8-C13	0.41687	22.54	0.27	0.070
		$\pi^*$ C17-C19	0.31643	20.13	0.29	0.069
$\pi$ C17-C19	1.65905	$\pi^*$ C8-C13	0.41687	21.54	0.27	0.069
		$\pi^*$ C14-C18	0.31529	19.31	0.29	0.067
LP (3) Br1	1.93144	$\pi^*$ C8-C13	0.41687	10.54	0.30	0.055
LP (1) N3	1.62271	$\pi^*$ O2-C7	0.30516	44.95	0.29	0.104
		$\pi^*$ N4-C6	0.26161	46.03	0.29	0.107

## 4. Conclusions

Inspired by the remarkable achievements of quinazoline derivatives in pharmacological activities, this study represents the outcomes of determination the chemical reactivity, thermodynamic parameters, and intramolecular interaction energies of 4 different quinazoline derivatives through the consideration of quantum chemical methods. The first stage of computational research is to determine the stable structure of the molecular system under study. Therefore, first of all, the theoretical structural factors and experimental structural factors of the derivatives optimized using the DFT/B3LYP/6-311++G (d, p) methodology were compared and found to be in accord. The values of thermodynamic parameters obtained from the calculations reveal that halogen substitution is preferable and all compounds examined are more polarized in aqueous media. In HOMO-LUMO analysis, the highest energy gap value was observed for compound Q3 in the vacuum phase with 5.005 eV. The changes caused by the substituents and solvent phases in the ESP maps were shown using a consistent color scheme. From SwissADME evaluation, the order of average  $\log P_{ow}$  of Q1-Q4 was determined as Q4 (3.32) > Q2 (3.24) > Q3 (3.23) > Q1 (2.96). The calculated  $\log P_{ow}$  values revealed that all studied compounds could exhibit lipophilic character. In addition, Molinspiration analysis suggests that the quinazoline ring and substituted phenyl ring provide the lipophilicity; carbonyl oxygen behaves as H-bond acceptor. It has been demonstrated through MLP maps that the substituents on the aromatic ring support lipophilic interactions. Investigating the substituent and/or solvent effects of structurally related molecules such as Q1-Q4 through quantum chemical methods, as well as expressing the obtained findings using both mathematical and visual language, emphasize the broader impact of the computational approach. Lastly, using NBO analyzes in conjunction with MEP map representations has been a very effective approach. It is observed that the  $\pi$ - $\pi^*$  interactions are predominant for each compound.

## Acknowledgments

The numerical calculations reported in this paper were partially performed at TUBITAK ULAKBIM, High Performance and Grid Computing Center (TRUBA resources).

## Author Contributions

Sümeyya Serin: Conceptualization, Methodology, Data curation, Writing – original draft, Writing – review & editing.

## References and Notes

- [1] Dua, R.; Shrivastava, S.; Sonwane, S. K.; Srivastava, S. K. *Adv. Biol. Res.* **2011**, *5*, 120.
- [2] Duró, C.; Jernei, T.; Szekeres, K.J.; Láng, G.G.; Oláh-Szabó, R.; Bószos, S.; Szabó, I.; Hudecz, F.; Csámpai, A. *Molecules* **2022**, *27*, 6758. [\[Crossref\]](#)
- [3] Fan, C.; Zhong, T.; Yang, H.; Yang, Y.; Wang, D.; Yang, X.; Xu, Y.; Fan, Y. *Eur. J. Med. Chem.* **2020**, *190*, 112108. [\[Crossref\]](#)
- [4] Shagufta; Ahmad, I. *Med. Chem. Commun.* **2017**, *8*, 871. [\[Crossref\]](#)
- [5] Auti, P. S.; George, G.; Paul, A. T. *RSC Adv.* **2020**, *10*, 41353. [\[Crossref\]](#)
- [6] Haider, K.; Das, S.; Joseph, A.; Yar, M.S. *Drug Dev. Res.* **2022**, *83*, 859. [\[Crossref\]](#)
- [7] Zayed, M. F.; Ibrahim, S.; Habib, E. E.; Hassan, M. H.; Ahmed, S.; Rateb, H. S. *J. Med. Chem.* **2019**, *15*, 657. [\[Crossref\]](#)
- [8] Santos-Ballardo, L.; García-Páez, F.; Picos-Corrales, L.A.; Ochoa-Terán, A.; Bastidas, P.; Calderón-Zamora, L.; Rendón-Maldonado, G.; Osuna-Martínez, U.; Sarmiento-Sánchez, J. I. *J. Chem. Sci.* **2020**, *132*, 100. [\[Crossref\]](#)
- [9] Jain, R. K.; Kashaw, V. *Asian J. Pharm. Pharmacol.* **2018**, *4*, 644. [\[Crossref\]](#)
- [10] Ji, Q.; Yang, D.; Wang, X.; Chen, C.; Deng, Q.; Ge, Z.; Yuan, L.; Yang, X.; Liao, F. *Bioorg. Med. Chem.* **2014**, *22*, 3405. [\[Crossref\]](#)
- [11] Ugale, V. G.; Bari, S. B. *Eur. J. Med. Chem.* **2014**, *80*, 447. [\[Crossref\]](#)
- [12] El-Azab, A. S.; El-Tahir, K. E. H. *Bioorg. Med. Chem. Lett.* **2012**, *22*, 1879. [\[Crossref\]](#)
- [13] Noureldin, N. A.; Kothayer, H.; Lashine, E. M.; Baraka, M. M.; El-Eraky, W.; Awdan, S. A. *Arch. Pharm. Chem. Life Sci.* **2017**, *350*, e1600332. [\[Crossref\]](#)
- [14] El-Azab A.S.; El-Tahir K. E. H. *Med. Chem. Res.* **2012**, *21*, 3785. [\[Crossref\]](#)
- [15] Cheke, R. S.; Shinde, S. D.; Ambhore, J. P.; Chaudhari, S. R.; Bari, S. B. *J. Mol. Struct.* **2022**, *1248*, 131384. [\[Crossref\]](#)
- [16] Kashaw, S. K.; Kashaw, V.; Mishra, P.; Jain, N. K.; Stables, J. P. *Eur. J. Med. Chem.* **2009**, *44*, 4335. [\[Crossref\]](#)
- [17] Fong, C.W. *Eur. J. Med. Chem.* **2014**, *85*, 661. [\[Crossref\]](#)

- [18] Hansch, C.; Björkroth, J. P.; and Leo, A. *J. Pharm. Sci.* **1987**, *76*, 663. [Crossref]
- [19] Michalik, M.; Lukes, V. *Acta Chim. Slovaca* **2016**, *9*, 89. [Crossref]
- [20] Du, Q.; Artega, G. A.; Mezey, P. G. *J. Comput. Aided. Mol. Des.* **1997**, *11*, 503. [Crossref]
- [21] Daina, A.; Michielin, O.; Zoete, V. *Sci. Rep.* **2017**, *7*, 1. [Crossref]
- [22] Molinspiration Cheminformatics free web services, <https://www.molinspiration.com>, Slovensky Grob, Slovakia.
- [23] Gaillard, P.; Carrupt P. A.; Testa B.; Boudon A. *J. Comput. Aided Mol. Des.* **1994**, *8*, 83. [Crossref]
- [24] Frisch, M. J.; Trucks, G. W.; Schlegel, H. B.; Scuseria, G. E.; Robb, M. A.; Cheeseman, J. R.; Scalmani, G.; Barone, V.; Petersson, G. A.; Nakatsuji, H.; Li, X.; Caricato, M.; Marenich, A. V.; Bloino, J.; Janesko, B. G.; Gomperts, R.; Mennucci, B.; Hratchian, H. P.; Ortiz, J.V.; Izmaylov, A. F.; Sonnenberg, J. L.; Williams Young, D.; Ding, F.; Lipparini, F.; Egidi, F.; Goings, J.; Peng, B.; Petrone, A.; Henderson, T.; Ranasinghe, D.; Zakrzewski, V. G.; Gao, J.; Rega, N.; Zheng, G.; Liang, W.; Hada, M.; Ehara, M.; Toyota, K.; Fukuda, R.; Hasegawa, J.; Ishida, M.; Nakajima, T.; Honda, Y.; Kitao, O.; Nakai, H.; Vreven, T.; Throssell, K.; Montgomery, J. A. Jr.; Peralta, J. E.; Ogliaro, F.; Bearpark, M. J.; Heyd, J. J.; Brothers, E. N.; Kudin, K. N.; Staroverov, V. N.; Keith, T. A.; Kobayashi, R.; Normand, J.; Raghavachari, K.; Rendell, A. P.; Burant, J. C.; Iyengar, S. S.; Tomasi, J.; Cossi, M.; Millam, J. M.; Klene, M.; Adamo, C.; Cammi, R.; Ochterski, J. W.; Martin, R. L.; Morokuma, K.; Farkas, O.; Foresman, J. B.; Fox, D. J. *Gaussian 16 Rev. C.01*, Wallingford, CT 2016.
- [25] Becke, A. D. *J. Chem. Phys.* **1993**, *98*, 1372. [Crossref]
- [26] Lee, C.; Yang, W.; Parr, R. G. *Phys. Rev. B* **1988**, *37*, 785. [Crossref]
- [27] Becke, A. D. *J. Chem. Phys.* **1993**, *98*, 5648. [Crossref]
- [28] Dennington, R.; Keith, T. A.; Millam, J. M. *GaussView*, Version 6 Semichem Inc., Shawnee Mission, KS. 2016.
- [29] O'Boyle, N. M.; Tenderholt, A. L.; Langer, K. M. *J. Comp. Chem.* **2008**, *29*, 839. [Crossref]
- [30] Cossi, M.; Rega, N.; Scalmani, G.; Barone, V. *J. J. Comput. Chem.* **2003**, *24*, 669. [Crossref]
- [31] McQuarrie, D. A. *Statistical thermodynamics*, Harper & Row Publishers, New York, 1973.
- [32] Hill, T. L. *An introduction to statistical thermodynamics*, Addison- Wesley Publishing, Inc, London, 1962.
- [33] Herzberg, G. *Molecular Spectra and Molecular Structure III*, 1. Edition, D. Van Nostrand Company, Inc., New York, 1964.
- [34] Serdaroğlu, G.; Durmaz, S. DFT and statistical mechanics entropy calculations of diatomic and polyatomic molecules, *Indian J. Chem.* **2010**, *49*, 866.
- [35] Koopmans, T. *Physica* **1934**, *1*, 104. [Crossref]
- [36] Parr, R. G.; Pearson, R. G. *J. Am. Chem. Soc.* **1983**, *105*, 7512. [Crossref]
- [37] Pearson, R. G. *Proc. Natl. Acad. Sci. U.S.A* **1986**, *83*, 8440. [Crossref]
- [38] Parr, R. G. *J. Am. Chem. Soc.* **1999**, *121*, 1922. [Crossref]
- [39] Perdew, J. P.; Levy, M. *Phys. Rev. Let.* **1983**, *51*, 1884. [Crossref]
- [40] Perdew, J. P.; Parr, R. G.; Levy, M.; Balduz, J. L. *Phys. Rev. Let.* **1982**, *49*, 1691. [Crossref]
- [41] Weinhold, F.; Landis, C. R.; Glendening, E. D. *Int. Rev. Phys. Chem.* **2016**, *35*, 399. [Crossref]
- [42] Reed, A. E.; Curtiss, L. A.; Weinhold, F. *Chem. Rev.* **1988**, *88*, 899. [Crossref]
- [43] Chen, S. C.; Yin, F. H.; Chen, Q.; Liu, Q.; He, M. Y. *Acta Cryst.* **2007**, *E63*, o3109. [Crossref]
- [44] Uzzaman, M.; Hasan, Md. K.; Mahmud, S.; Yousuf, A.; Uddin, S. I. M. N.; Barua, A. *Inform. Med. Unlocked* **2021**, *25*, 100706. [Crossref]
- [45] Murray, J. S.; Politzer, P. *Wiley Interdiscip. Rev. Comput. Mol. Sci.* **2011**, *1*, 153. [Crossref]
- [46] Murray, J. S.; Sen, K. *Molecular electrostatic potentials: concepts and applications*, first ed., Elsevier, Amsterdam, 1996.
- [47] Van De Waterbeemd, H.; Gifford, E. *Nat. Rev. Drug Discov.* **2003**, *2*, 192. [Crossref]
- [48] Cheng, T.; Zhao, Y.; Li, X.; Lin, F.; Xu, Y.; Zhang, X.; Li, Y.; Wang, R. *J. Chem. Inf. Model.* **2007**, *47*, 2140. [Crossref]
- [49] Daina, A.; Michielin, O.; Zoete, V. *J. Chem. Inf. Model.* **2014**, *54*, 3284. [Crossref]
- [50] Wildman, S. A.; Crippen, G. M. *J. Chem. Inf. Comput. Sci.* **1999**, *39*, 868. [Crossref]
- [51] Lipinski, C. A.; Lombardo, F.; Dominy, B. W.; Feeney, P. *J. Adv. Drug Deliv. Rev.* **2001**, *46*, 3. [Crossref]
- [52] Silicos-it. (n.d.). Retrieved from <https://www.silicos-it.be>

## How to cite this article

Serin, S. *Orbital: Electron. J. Chem.* **2024**, *16*, 30. DOI: <http://dx.doi.org/10.17807/orbital.v15i5.18934>